BIOCHEMISTRY
including biophysical chemistry & molecular biology

Article

pubs.acs.org/biochemistry

Effect of Temperature on the Intrinsic Flexibility of DNA and Its Interaction with Architectural Proteins

Rosalie P. C. Driessen,[†] Gerrit Sitters,[‡] Niels Laurens,[‡] Geri F. Moolenaar,[†] Gijs J. L. Wuite,[‡] Nora Goosen,[†] and Remus Th. Dame*[,†]

[†]Molecular Genetics, Leiden Institute of Chemistry and Cell Observatory, Leiden University, 2333 CC Leiden, The Netherlands
[‡]Department of Physics and Astronomy, VU University, 1081 HV Amsterdam, The Netherlands

Supporting Information

ABSTRACT: The helical structure of double-stranded DNA is destabilized by increasing temperature. Above a critical temperature (the melting temperature), the two strands in duplex DNA become fully separated. Below this temperature, the structural effects are localized. Using tethered particle motion in a temperature-controlled sample chamber, we systematically investigated the effect of increasing temperature on DNA structure and the interplay between this effect and protein binding. Our measurements revealed that (1) increasing temperature enhances DNA flexibility, effectively leading to more compact folding of the double-stranded DNA chain, and (2) temperature differentially affects different types of DNA-bending chromatin proteins from mesophilic and thermophilic organisms. Thus, our findings aid in understanding genome organization in organisms thriving at moderate as well as extreme temperatures. Moreover, our results underscore the importance of carefully controlling and measuring temperature in single-molecule DNA (micromanipulation) experiments.

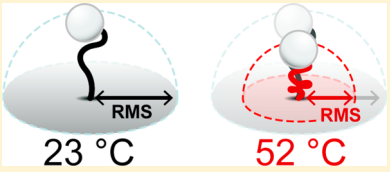

Double-stranded DNA (dsDNA) is a semiflexible polymer.[1] On short length scales (on the order of its persistence length, ~150 bp or ~50 nm), stiffness dominates its conformation and bending is energetically unfavorable. However, on a larger scale, dsDNA acts as a flexible polymer and forms a random coil. Although the exact cause of DNA rigidity remains unclear, it has been proposed that both base pair stacking and the electrostatic repulsions of the negatively charged phosphate backbone contribute to the local stiffness of the DNA.[1,2] To facilitate genome-based processes such as transcription, DNA repair, and replication, the relatively stiff DNA is sharply bent on local scales.[3] Despite its global flexibility, genomic DNA is also bent substantially to fit into the volume of a cell or cell nucleus. Across all domains of life, cells employ small architectural proteins that bend the DNA to compact the genome.[4] Eukaryotes and many archaeal species express histone proteins that sharply bend and wrap DNA into nucleosomes.[5−7] Other architectural proteins have been shown to induce compaction by local DNA bending. Examples include eukaryotic high-mobility group (HMG) proteins,[8] the bacterial DNA bending proteins HU, IHF, and Fis,[9,10] and the crenarchaeal proteins Sul7 and Cren7.[11] Besides the role of DNA-bending proteins in genome compaction and organization, the bending induced by these proteins is also crucial in regulatory processes.[12] Regulatory complexes *in vivo* often involve the formation of small DNA loops[13] that require sharp bending of the DNA. A mechanism for enhancing the formation and stability of these loops is the binding of a DNA-bending protein within the loop. For example, HU was shown to stabilize various kinds of transcriptional repression loops (among which loops mediated by the bacterial Lac and Gal repressor) by enhancing DNA flexibility.[14−17] In the Gal repressosome, two GalR dimers form a small loop facilitated by the binding of an HU dimer at the apex of the loop.[18] Other studies have shown that sharp bending of DNA can occur spontaneously, yielding a higher intrinsic bendability of DNA on short length scales compared to that on long length scales.[19,20] Such strong bending of short dsDNA is caused by the formation of either small melting bubbles or transient kinks.[21−25] On the basis of the observation that sharp bending of DNA occurs spontaneously, it was suggested that DNA flexibility itself acts as a factor affecting the conformation and stability of looped regulatory complexes *in vivo*.[26]

It is likely that the flexibility and bendability of DNA affect spatial genome folding and functioning. Indeed, it has been shown in biochemical ensemble measurements that temperature directly affects DNA structure by changing its persistence length.[27] Besides such a direct effect on DNA structure, temperature might also influence the interactions between DNA and architectural proteins, and hence chromatin structure. Growth temperature and fluctuations in this temperature are thus expected to have a strong impact on *in vivo* DNA organization and gene regulation. Indeed, the transcription of many genes changes following moderate temperature shifts in both mesophilic *Escherichia coli*[28] and thermophilic *Sulfolobus solfataricus*.[29] In addition to being associated with a general stress response,[30] such effects on transcription could in part be mediated by global changes in

Received: March 20, 2014
Revised: September 10, 2014
Published: October 7, 2014

   dx.doi.org/10.1021/bi500344j | *Biochemistry* 2014, 53, 6430−6438

chromatin structure caused by the change in temperature. Single-molecule experiments concerning DNA flexibility and protein−DNA interactions are generally conducted at room temperature. However, a large majority of organisms live at temperatures different from room temperature: psychrophiles thrive at temperatures around 0 °C, mesophiles at temperatures from 20 to 45 °C, while thermophilic organisms at temperatures up to ∼100 °C. In this study, we investigate the effect of temperature on DNA structure and flexibility at temperatures ranging from 23 to 52 °C using a temperature-controlled tethered particle motion (TPM) setup. Moreover, we investigate the effect of temperature on the binding and bending behavior of the architectural proteins Cren7 and Sul7 from the thermophilic organism *S. solfataricus* (living at temperatures between 40 and 90 °C) and HU from mesophilic *E. coli* (living at temperatures between 10 and 40 °C).

EXPERIMENTAL PROCEDURES

Protein Purification. Cren7 was purified as described previously.[11] The Sul7 protein was purified from *E. coli* strain BL21-CodonPlus(DE3) containing plasmid pRD26 [a pET11a derivative containing the gene encoding Sul7 (gene SSO10610) from *S. solfataricus*]. Cells were grown in Luria-Bertani (LB) medium up to an OD_{600} of ≈0.4, and expression was induced using 0.5 mM isopropyl β-D-1-thiogalactopyranoside at 37 °C. Two hours after induction, cells were harvested by centrifugation and resuspended in 20 mL of buffer A [50 mM Tris-HCl (pH 8.0), 2 mM $MgCl_2$, 0.1% Triton X-100, 386 μg/mL benzamidine hydrochloride, and 10 mM β-mercaptoethanol]. Cells were lysed by sonication; 1000 units of OmniCleave Endonuclease (Westburg) was added per gram of cells, and the cell lysate was incubated for 30 min at room temperature. After the cell lysate had been heated for 40 min at 70 °C, 1 mL of 0.5 M EDTA was added. The cell lysate was centrifuged for 30 min at 37000 rpm and filtered through a 0.45 μm membrane filter (Millipore). The supernatant was applied to a HiTrap-S column (GE Healthcare), equilibrated in buffer B [10 mM KPO_4 (pH 7.0) and 10% glycerol]. Protein was eluted with a linear gradient from 0 to 1 M NaCl in buffer B. Cren7 and Sul7 proteins were dialyzed at 4 °C against a storage buffer [20 mM HEPES (pH 7.5), 100 mM NaCl, 10% glycerol, and 10 mM β-mercaptoethanol] and stored at −80 °C until they were required. Protein concentrations were determined using a bicinchoninic acid (BCA) protein assay (Thermo Scientific). HU protein was purified as described previously.[31]

DNA Substrates. End-labeled DNA substrates of 685 bp with different GC contents (32, 53, and 70% GC) were generated by polymerase chain reaction (PCR) using plasmids pRD118, pNP83,[32] and pBTH154 as templates and biotin- and digoxygenin-labeled primers (designed to specifically yield a product of the desired length based on the sequences cloned into these plasmids). pRD118 was constructed by inserting a 685 bp fragment from the *S. solfataricus* P2 genome[33] into the *Nde*I and *Bam*HI site of pET3-his.[34] pBTH154 was constructed by inserting the *dasR* gene (SCO5231) of *Streptomyces coelicolor* A3(2)[35] into the *Xba*I and *Xma*I site of pUT18C (Euromedex). All PCR products were purified using a GenElute PCR Clean-up kit (Sigma-Aldrich). DNA substrates were analyzed in relation to the local GC percentage and predicted curvature (see Figure S1 of the Supporting Information) to ensure the variation is small and to prevent local curvature from dominating the global flexibility of the substrates. DNA substrates used for the bulk melting experiments were obtained following the same approach with unlabeled primers.

Bulk Melting Curves. Melting curves of the three DNA substrates with different GC contents (see above) were obtained using a Varian Cary300Bio UV−vis spectrophotometer, measuring ultraviolet absorbance at λ = 260 nm. The DNA was diluted to a final concentration of 4 μg/mL in a buffer containing 10 mM HEPES (pH 7.5) and 100 mM NaCl. The temperature was increased at a rate of 1 °C/min from 25 to 95 °C. The melting temperature (T_m) is defined as the temperature at which half of the dsDNA is dissociated into ssDNA, which equals the temperature at which the slope of the melting curve is maximal. To determine the T_m, the first derivative was calculated and the peak position (corresponding to the T_m) was determined by fitting a Gaussian distribution.

Tethered Particle Motion Experiments. Flow cells (volume of ∼30 μL) were incubated with 20 μg/mL anti-DIG antibodies (Roche) for 5 min. Passivation of the surface was achieved by flushing the flow cell with 0.4% (w/v) Blotting grade Blocker (BGB) (Bio-Rad) in buffer I [10 mM Tris (pH 7.5), 150 mM NaCl, 1 mM EDTA, 1 mM DTT, 3% glycerol, and 100 μg/mL acetylated BSA (Ambion)] and incubating the sample for 15 min at the desired temperature (23−52 °C). The flow cell was flushed with buffer I, filled with a 200 pM DNA solution (functionalized with biotin and DIG), incubated for 10 min, and flushed again with buffer I. Streptavidin-coated polystyrene beads with a diameter of 0.46 μm [1% (w/v) (G Kisker)] were diluted 300 times in buffer I, flushed into the flow cell, and incubated for 10 min to allow binding to the biotin ends of the DNA. The flow cell was washed with protein diluted in buffer II [10 mM HEPES (pH 7.5), 100 mM NaCl, and 0.2% (w/v) BGB] for Cren7 and Sul7 or buffer III [20 mM HEPES (pH 7.9), 60 mM KCl, and 0.2% (w/v) BGB] for HU at the desired temperature. After the final incubation solution with or without protein had been added, the flow cell was closed and incubated at the desired temperature (23−52 °C) for 10 min before the measurements were started. Experiments without protein were all conducted in buffer II.

Tethered particle motion experiments were performed on an inverted Nikon microscope (Diaphot 300), using a 100× oil-immersion objective (NA = 1.25). To control the temperature of the flow cell, a custom-built temperature control system was implemented by placing heating elements around the objective and inside the flow cell holder (see Figure S2 of the Supporting Information for details). A feedback system was used to secure a constant temperature within ±1 °C. Using a calibrated temperature probe at the top glass slide of the flow cell, the temperature was calibrated. The sample stage was isolated to keep the temperature stable within the sample. Images were acquired using a CMOS camera (Thorlabs) at 25 Hz, with a camera exposure time of 20 ms. The x and y coordinates of individual beads were tracked in real time by custom-developed LabView software (National Instruments) as described previously.[36] Typical data obtained for a DNA-tethered bead are shown in Figure S3 of the Supporting Information.

Data Analysis. The root-mean-square (rms) value of the excursion of each individual bead was calculated from x and y coordinates of a 40 s time trace (corrected for linear drift) by the equation $\text{rms} = [\langle (x - \bar{x})^2 + (y - \bar{y})^2 \rangle]^{1/2}$, where $\bar{x}$ and $\bar{y}$ are averaged over the full time trace. Symmetry of the excursion of the tethered beads was evaluated by calculating the anisotropic ratio $a = l_{major}/l_{minor}$ from the xy scatter plots, where l_{major} and l_{minor} represent the major and minor axes of the

dx.doi.org/10.1021/bi500344j | Biochemistry 2014, 53, 6430−6438

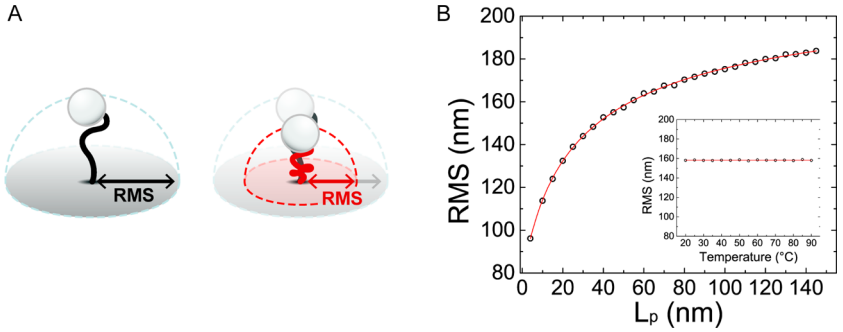

Figure 1. rms is a measure of DNA persistence length. (A) Schematic representation of a TPM experiment. In the left panel, the rms value quantifies the excursion of a bead attached to a single DNA molecule, tethered to the surface of the flow cell. The right panel shows that as the persistence length decreases, the DNA molecule will be in a more compact configuration (red DNA molecule), which leads to a smaller rms value. (B) Dependence of rms on persistence length L_p obtained from bead movement simulations (L_0 = 233 nm, and d_{bead} = 460 nm) fitted with eq 2. The inset shows that the bead movement (rms) itself is not affected by temperature when DNA parameters are kept constant (L_0 = 233 nm, L_p = 50 nm, and d_{bead} = 460 nm).

xy scatter plot, respectively. Fluctuations of rms with time were quantified by calculating the relative standard deviation of the smoothed rms ($\sigma_{rel} = \sigma_{smoothed}/\langle rms\rangle_{smoothed}$, where $\sigma_{smoothed}$ represents the standard deviation of $rms_{smoothed}$), which represents the rms smoothed over a 2 s time window. Only tethers with high symmetry ($a \leq 1.14$) and small rms fluctuations ($\sigma_{rel} \leq 0.06$) were classified as good tethers and selected for further analysis (see Figure S4 of the Supporting Information for a typical rms distribution of a measurement of all tethers and selected tethers). For each measured condition, rms values were obtained by fitting a single Gaussian to the histogram of the rms values of individual tethers (N = 52−352).

Bead Movement Simulations. Bead movement is simulated numerically by solving the Langevin equation for a tethered bead. This is done for both translation and rotation:[37]

$$x_{n+1} = x_n + (\gamma - 1)F_{ext} + F_{brown}\Delta t$$
$$\phi_{n+1} = \phi_n + (\beta - 1)\Theta_{DNA} + \Theta_{brown}\Delta t \quad (1)$$

where x_n and x_{n+1} are the bead's three-dimensional positions at steps n and $n + 1$ of the simulation, respectively. Angles φ_n and φ_{n+1} denote the bead's orientation. γ and β are the effective translational and rotational drag coefficient vectors, respectively, which are calculated using Faxén's law:[38]

$$\gamma_x = \gamma_y = \frac{\gamma_0}{1 - \frac{9}{16}\left(\frac{R}{z}\right) + \frac{1}{8}\left(\frac{R}{z}\right)^3} \qquad \gamma_z = \frac{\gamma_0}{1 - \frac{9}{8}\left(\frac{R}{z}\right) + \frac{1}{2}\left(\frac{R}{z}\right)^3}$$
$$\beta_x = \beta_y = \frac{\beta_0}{1 - \frac{1}{8}\left(\frac{R}{z}\right)^3} \qquad \beta_z = \frac{\beta_0}{1 - \frac{5}{16}\left(\frac{R}{z}\right)^3 + \frac{15}{256}\left(\frac{R}{z}\right)^6}$$

where $\gamma_0 = (6\pi\eta R\ dx/dt)$ and $\beta_0 = (8\pi\eta R^3\ d\varphi/dt)$, the translational and rotational drag coefficients, respectively, in bulk with η de viscosity of the medium (see Figure S5 of the Supporting Information). R is the bead radius, and z is the axial distance between the surface and bead center. F_{ext} values are the external forces working on the bead caused by gravity, buoyancy, the surface, and the DNA:

$$\vec{F}_{buoyancy} + \vec{F}_{gravity} = \frac{4}{3}\pi R^3 g(\rho_{med} - \rho_{bead})\hat{z}$$
$$\vec{F}_{surface} = 4\pi\varepsilon_w\varepsilon_0\psi_0^2 Re^{-(z-R)/l}\hat{z}$$

where g represents the gravitational constant, ρ_{med} represents the density of water, ρ_{bead} represents the density of the bead, ε_w and ε_0 represent the permittivity of water and vacuum, respectively, ψ_0 represents the effective surface potential, and l represents the Debye screening length.[39] See Table S1 of the Supporting Information for the parameters used. Θ_{DNA} is the torque exerted on the bead caused by the DNA. The DNA is modeled by the finite WLC model assuming fully constraint boundary conditions.[40] F_{brown} and Θ_{brown} are the fluctuating thermal force and torque, respectively, that are described by the fluctuation−dissipation theorem and are Gaussian distributed with the following properties:[41]

$$\langle F_{brown}\rangle = 0 \quad \sigma_{F_{brown}} = \sqrt{\frac{2\gamma k_B T}{\Delta t}}$$
$$\langle T_{brown}\rangle = 0 \quad \sigma_{T_{brown}} = \sqrt{\frac{2\beta k_B T}{\Delta t}}$$

where Δt is the time step of the simulation and is typically set to 1 μs. A decreasing Δt did not affect the statistical properties of the simulated traces.

RESULTS

Increasing Temperature Enhances DNA Flexibility. The motivation for our studies was to study protein−DNA interactions at temperatures relevant for the organisms encoding these proteins. Such interactions might be affected by changes in structure and DNA flexibility occurring with a change in temperature. To investigate the direct effect of temperature on DNA structure and flexibility, we performed tethered particle motion (TPM) experiments over a range of temperatures. Because the physical properties of dsDNA are dependent on the base pair composition,[42] we measured three different DNA substrates identical in length (685 bp) but different in average GC content (32, 53, and 70%). Using bulk DNA melting measurements, we first determined the melting temperatures (T_m) to be $T_{m,32\%}$ = 76.8 ± 0.5 °C, $T_{m,53\%}$ = 84.9 ± 0.5 °C, and $T_{m,70\%}$ = 91.2 ± 0.5 °C for the substrate with 32, 53, and 70% GC base pairs, respectively (see Figure S6 of the Supporting Information). In our TPM experiments, we focus on the local effects of temperature on global DNA conformation by measuring at temperatures below the melting temperature of all three DNA substrates (23−52 °C). We probed the conformational state of many individual DNA

dx.doi.org/10.1021/bi500344j | Biochemistry 2014, 53, 6430−6438

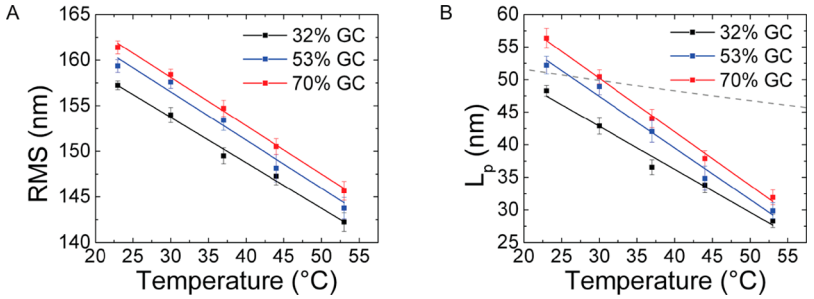

Figure 2. TPM measurements of temperature-dependent DNA flexibility. (A) rms distances of dsDNA molecules (685 bp) with GC percentages of 32, 53, and 70% as a function of temperature. Error bars represent the standard error of the mean (N = 58−352). (B) Apparent persistence length of all three substrates as a function of temperature. L_p is calculated from data shown in panel A using eq 2. Lines are linear fits to the data points (see Table 1 for fitting parameters). The dashed gray line represents the theoretical temperature dependence of the persistence length of a chain [$L_p = A/(k_BT)$].

molecules in this range of temperatures by tracking the excursion of the attached bead [quantified by the root-mean-square (rms) value of its excursion]. If the length of a tether is not changed, the rms of the attached bead is a measure of its apparent persistence length; a tether attains a more compact formation if it becomes more flexible or if it is locally bent by a ligand (see Figure 1A). At 23 °C, the measured rms values ranged from 157.2 ± 0.5 nm [the error represents the standard error of the mean (SE)] for the 32% GC substrate to 161.4 ± 0.7 nm for the 70% GC substrate. DNA with a higher GC content yielded a slightly higher rms value, because of an on average somewhat less flexible DNA substrate. Increasing the temperature caused the rms values of all DNA tethers to decrease (see Figure 2A), pointing to an increase in flexibility. To quantitatively relate the measured RMS values to the physical properties of the DNA, we performed numerical simulations describing the movement of the bead as a function of DNA persistence length (L_p). The rms of the simulated tethered beads was calculated from the x and y positions obtained from the simulations (see Experimental Procedures). Figure 1B shows the relation between the persistence length and the measured rms value for a tether with a contour length (L_0) of 233 nm (685 bp) and a bead diameter (d_{bead}) of 460 nm. By fitting the results with a hyperbola function, we obtained the following empirical relation between L_p and rms:

$$\text{rms} = 233 - \frac{156}{(1 + 0.08L_p)^{0.45}} \quad (2)$$

To validate our approach and to ensure that the measured change in rms is exclusively due to changes in the flexibility of the DNA, we tested if the temperature has an effect on the bead motion itself. In our simulations, a change in temperature may affect the movement of the bead by influencing the viscosity of the solution and the thermal fluctuations on the bead and the DNA. Despite these temperature effects, the bead movement (L_0 = 233 nm, L_p = 50 nm, and d_{bead} = 460 nm) yielded a constant rms value at different temperatures (see the inset of Figure 1B), which indicates that the rms itself is not influenced by temperature within a range of 20−90 °C. This confirms that the measured rms is dependent only on the physical properties of the DNA, which we can describe as a function of apparent persistence length according to eq 2. The apparent persistence length of the DNA molecule is a measure for the average flexibility of a heterogeneous chain.[43,44] Using eq 2, we calculated the apparent persistence length of the DNA substrates within the measured temperature range. Figure 2B shows that the apparent persistence length scales linearly with temperature within this temperature range. This temperature dependence is much stronger than the theoretical temperature dependency of the persistence length of the polymer [$L_p = A/(k_BT)$, where A is the bending stiffness and k_B the Boltzmann constant (see the gray dashed line)], indicating a structural change in the DNA double helix. Linear fitting of the data ($L_p = L_p^0 - CT$) yielded a temperature dependence of the persistence length (C), which is slightly dependent on the GC percentage of the DNA substrate (see Table 1). L_p^0 denotes the apparent persistence length at 0 °C, but as water will freeze around this temperature, this linear dependence is not valid at temperatures close to 0 °C. The generic effect of temperature on DNA flexibility is in agreement with recent magnetic tweezers studies.[45,46] The observed linear dependence of the apparent persistence length on temperature is in good qualitative agreement with the work of Geggier et al.,[27] in which cyclization of short DNA fragments was investigated in the range of 5−42 °C in ensemble measurements.

Table 1. Temperature-Dependent DNA Properties of DNA Substrates (685 bp) with Different GC Contents[a]

GC content of DNA substrate (%)	C (nm/°C)	L_p^0 (nm)	T_m (°C)
32	0.66 ± 0.05	62.7 ± 1.9	76.8 ± 0.5
53	0.79 ± 0.05	71.2 ± 2.3	84.9 ± 0.5
70	0.82 ± 0.03	74.9 ± 1.2	91.2 ± 0.5

[a]The errors in the values of C and L_p^0 indicate the uncertainty in the linear fit to the experimental data.

Influence of Temperature on the Binding and Bending of DNA-Bending Proteins. A higher flexibility of DNA at higher temperatures could be an important element contributing to DNA organization and dynamics in organisms with high growth temperatures. As the apparent persistence length of DNA is reduced with an increase in temperature, the conformation of the molecule becomes more compact in a manner independent of architectural protein binding. In addition to such a direct effect of temperature on the intrinsic properties of DNA, the interaction between architectural proteins and DNA might also be affected by temperature. However, single-molecule experiments concerning protein−DNA interactions of architectural proteins have been traditionally conducted at room temperature. To determine the architectural properties of such proteins under conditions more relevant for the *in vivo* situation, we investigated the

dx.doi.org/10.1021/bi500344j | *Biochemistry* 2014, 53, 6430−6438

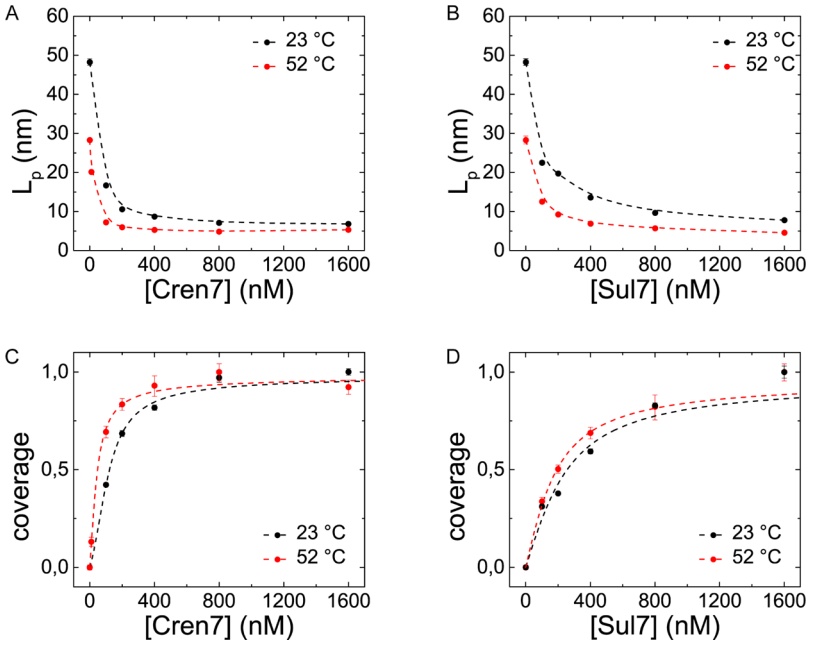

Figure 3. TPM measurements of the effect of temperature on protein−DNA binding. (A and B) Apparent persistence length as a function of protein concentration of Cren7 and Sul7 at 23 and 52 °C. (C and D) Fractional coverage as a function of protein concentration, calculated according to eq 3 from data shown in panels A and B. Fitting the coverage to the theory of McGhee and von Hippel showed that binding affinity is increased at 52 °C: for Cren7, $K_{Cren,23} = (2.5 \pm 0.2) \times 10^5$ nM^{-1} and $K_{Cren,52} = (7.4 \pm 1.4) \times 10^5$ nM^{-1}, and for Sul7, $K_{Sul,23} = (1.3 \pm 0.3) \times 10^5$ nM^{-1} and $K_{Sul,52} = (1.8 \pm 0.2) \times 10^5$ nM^{-1}. Error bars represent the standard error of the mean (N = 69−352).

effects of the DNA-bending proteins Cren7 and Sul7 from thermophilic *S. solfataricus* and HU from mesophilic *E. coli* on DNA structure at physiological temperatures.

Sulfolobus species[47,48] live at temperatures in the range of 40−90 °C.[49] The Cren7 and Sul7 proteins encoded by these organisms are structural homologues, both inducing rigid bends upon binding to DNA[11] by intercalating into the minor groove.[50−52] Our earlier single-molecule micromanipulation experiments performed at room temperature (~23 °C) revealed that this bending results in a decrease in the apparent persistence length and thus compaction of DNA molecules.[11] DNA melting experiments revealed that both Cren7 and Sul7 increase the melting temperature,[53,54] which might imply an important role for these proteins in maintaining DNA integrity at high temperatures. To determine how the interaction of Cren7 and Sul7 with DNA is affected by temperature in the submelting regime in which DNA becomes more flexible, we performed TPM experiments at both 23 and 52 °C. For these studies, we used the 32% GC substrate, which is representative for the average GC content of the *S. solfataricus* genome.[33] Persistence length L_p for protein concentrations of 0−1600 nM for both Cren7 and Sul7 at 23 and 52 °C, calculated from the measured rms values using eq 2, is shown in panels A and B of Figure 3 (see Figures S7 and S8 of the Supporting Information for rms values and typical rms distributions). For both proteins, a minimal persistence length of ~10 nm is reached at 23 °C, which is consistent with our earlier measurements using magnetic tweezers conducted at this temperature.[11] This agreement further validates our approach of converting rms values into values for persistence length L_p. At 52 °C, compaction sets in at protein concentrations lower than those at which compaction sets in at 23 °C, but the maximal level of compaction achieved at both temperatures is comparable. At high protein concentrations, when the DNA is saturated with protein, the change in temperature does not measurably influence the conformation of the protein−DNA complexes. To quantitatively compare the binding affinities of the proteins at the different temperatures, we calculated the fractional coverage (ν) of the DNA as follows:[55]

$$\nu = \frac{\sqrt{1/L_p} - \sqrt{1/L_{p,bare}}}{\sqrt{1/L_{p,saturated}} - \sqrt{1/L_{p,bare}}} \quad (3)$$

where L_p represents the measured persistence length, $L_{p,saturated}$ the minimal persistence length at saturation, and $L_{p,bare}$ the persistence length of bare DNA. In this approach, it is assumed that each bound protein makes an equal contribution to the decrease in DNA stiffness. Panels C and D of Figure 3 show the fractional coverage as a function of protein concentration. To calculate binding affinities under the different conditions, the fractional coverage was fit to the theory of McGhee and von Hippel.[56] This model describes the binding of protein to DNA in terms of the association constant (K), a cooperativity parameter (ω), and the protein binding site (n). Using a footprint of n = 8 bp for both proteins,[51,57] we obtained fitting parameters for K and ω. Both Cren7 and Sul7 bind the DNA substrate with higher affinity at 52 °C than at 23 °C. The association constant found for Cren7 equals $(2.5 \pm 0.2) \times 10^5$ nM^{-1} at room temperature (23 °C) ($K_{Cren,23}$) and increased to $(7.4 \pm 1.4) \times 10^5$ nM^{-1} at 52 °C ($K_{Cren,52}$). The cooperativity factor ($\omega_{Cren,23}$) of 18.8 ± 3.2 indicates low cooperativity in binding, which is somewhat affected by the increase in temperature as $\omega_{Cren,52}$ = 10.4 ± 3.6. Sul7 exhibits a DNA binding affinity lower than that of Cren7 as $K_{Sul,23} = (1.3 \pm 0.3) \times 10^5$ nM^{-1} at 23 °C and $K_{Sul,52} = (1.8 \pm 0.2) \times 10^5$ nM^{-1} at 52 °C, yielding a slightly higher binding affinity at 52 °C. Similar to that of Cren7, the cooperativity in binding of Sul7 to DNA is essentially independent of temperature: $\omega_{Sul,23}$ = 8.4 ± 2.4, and $\omega_{Sul,52}$ = 8.1 ± 2.0.

dx.doi.org/10.1021/bi500344j | *Biochemistry* 2014, 53, 6430−6438

To investigate whether the effect of temperature on DNA binding shown for Cren7 and Sul7 is generic for DNA-bending proteins, we performed similar experiments with the bacterial chromatin protein HU. HU is the most abundant DNA-bending protein in *E. coli*. It exhibits two different DNA binding modes depending on the stoichiometry: DNA bending and compaction at low protein concentrations and DNA stiffening at high protein concentrations.[43,58,59] TPM measurements performed at 23 °C show that HU induces compaction by reducing the apparent persistence length to a minimum of 12.9 ± 0.2 nm at a protein concentration of 400 nM (see Figure 4 and Figure S9 of the Supporting Information). At HU concentrations of >400 nM, the persistence length increases to 20.1 ± 0.4 nm at a protein concentration of 1600 nM, reflecting the transition into the stiffening mode. In this concentration regime, HU proteins bind side by side forming filaments, which stabilizes the DNA helix.[60] Force could, for example, facilitate close side-by-side binding of HU proteins along the DNA, which causes stiffening of the DNA. We did not observe an increase in persistence length above that of bare DNA as observed in previous micromanipulation experiments of single HU–DNA complexes.[43,58] However, previously reported TPM experiments exhibited a similar trend: the persistence length increases at high HU concentrations but does not exceed the persistence length of bare DNA molecules.[59] Possibly, the force applied in the previous DNA micromanipulation experiments facilitates the transition into the stiffening mode of HU, giving rise to the apparent discrepancy in observed persistence lengths. Next, we conducted TPM measurements for the same protein concentration range at 37 °C, the optimal growth temperature of *E. coli*. Surprisingly, a temperature increase of only 14 °C had a large effect on the measured apparent persistence length. Although the maximal level of compaction was achieved at a similar protein concentration (400 nM), the persistence length at this concentration was reduced significantly to 6.1 ± 0.2 nm at 37 °C. In the stiffening regime (>400 nM), the persistence length increased slightly to 10.7 ± 0.3 nm at 1600 nM, indicating that the DNA stiffening still occurs in this regime at 37 °C. As the maximal level of compaction is achieved at the same protein concentration, the affinity of HU for DNA is not affected by the change in temperature from 23 to 37 °C. The change in temperature did, however, significantly enhance the degree of compaction induced by HU, suggesting that the degree of bending induced by HU is increased at 37 °C.

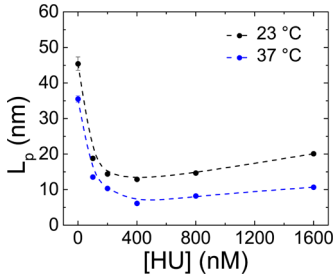

Figure 4. Apparent persistence length as a function of HU concentration at 23 and 37 °C. Compaction is increased at 37 °C. Error bars represent the standard error of the mean (N = 52–236).

DISCUSSION

Our single-molecule TPM experiments reveal that the flexibility of DNA strongly depends on temperature in the range of 23–52 °C. The temperature coefficient of the persistence length (C) is slightly dependent on the GC content of the DNA substrate and ranges from 0.66 ± 0.05 nm/°C for the DNA substrate with an average GC content of 32% to 0.82 ± 0.03 nm/°C for the substrate with a GC content of 70%. The temperature effect on the apparent persistence length observed in our study is much more pronounced than in previous work by Geggier et al.[27] As in our study, the work by Geggier et al. relies on an indirect readout of the temperature effect as they translate ring closure efficiencies of DNA substrates into persistence length using theoretical models. Moreover, the different experimental conditions (i.e., buffer conditions, especially $MgCl_2$ concentrations) may in part explain the difference in temperature dependency. Although it is thus hard to identify the nature of the quantitative difference, the observed trend is similar: an increased temperature lowers the resistance to bending of the DNA. What causes such a strong temperature dependence on the L_p remains unclear. The thermal stability of the dsDNA helix involves base pair interactions between bases of complementary strands and base stacking interactions between adjacent bases. Although Yakovchuk et al.[61] found that the base stacking interactions are the dominant factor in stabilizing the double-stranded helix, they did not show how this relates to the bending rigidity of the DNA. A recent study addressed this question by measuring mechanical properties of chemically modified DNA molecules, with altered charge or base stacking interactions.[62] This revealed that stacking interactions do not straightforwardly correlate with the mechanical properties of DNA, such as the persistence length. It is thus unlikely that stacking interactions alone cause such a pronounced temperature-dependent persistence length. Spontaneous sharp bending of dsDNA has been explained in different models involving kinks (caused by unstacking of adjacent base pairs) or small melting bubbles (disrupted base pairing and/or base stacking). Probably increasing temperature enhances both of these processes, strongly influencing the apparent persistence length (as observed in our experiments). A recent theoretical study indeed suggests a model that describes the experimentally observed temperature-dependent DNA persistence length as a function of both an isotropic temperature-dependent bending stiffness of the dsDNA helix and small local melting bubbles.[63]

The fact that the flexibility of dsDNA strongly depends on temperature has important implications for genome conformation *in vivo*. Organisms will experience different mechanical properties of DNA depending on the temperature of their natural habitat. As temperature increases the bendability of dsDNA, organisms living at elevated temperatures could benefit from this increased bendability in light of genome compaction. The persistence length directly relates to the size of an unconstrained dsDNA molecule in solution, typically quantified by the so-called radius of gyration (R_g). For instance, the genome of an archaeal or bacterial cell is on the order of millimeters in length, which corresponds to an R_g of ≈4 μm at 25 °C (L_p = 50 nm). A change in temperature to 52 °C would reduce the radius of gyration of a genome of that length to ≈3.2 μm (a reduction in effective volume of ∼25%). Temperature itself could thus serve as a mechanism to aid in compacting the genomic DNA. It is therefore an important aspect to consider

dx.doi.org/10.1021/bi500344j | *Biochemistry* 2014, 53, 6430–6438

when studying *in vivo* chromatin organization and compaction of thermophilic organisms and psychrophilic organisms living at temperatures that differ from room temperature.

Our results show that temperature not only affects the intrinsic properties of DNA but also influences protein−DNA interactions of DNA-bending proteins. Interestingly, this temperature dependence is not shared among the different DNA-bending proteins investigated; it seems to depend on the nature of the protein−DNA interactions. Both Cren7 and Sul7 from thermophilic *S. solfataricus* exhibit an increased binding affinity at an elevated temperature of 52 °C. Increased binding affinity at higher temperatures was shown before for Sul7 by isothermal titration calorimetry (ITC).[64,65] In these ITC studies, the binding affinity for poly(dGdC) increased ∼5-fold with an increase in temperature from 25 to 80 °C. Molecular dynamics simulations of Cren7 also showed an increased affinity at elevated temperatures.[66] The increase in binding affinity could be attributed to the increased flexibility of DNA at higher temperatures, which lowers the energy barrier to induce DNA bending. Another mechanism, which could contribute to an increased affinity, is one in which transient melting bubbles make the DNA more accessible for binding of Cren7 and Sul7, as these proteins intercalate into the minor groove of DNA.

In contrast with Cren7 and Sul7, the DNA-bending protein HU from mesophilic *E. coli* did not show an increased binding affinity upon an increase in temperature (ΔT) of 14 °C. Instead, HU binding at 37 °C resulted in significantly enhanced compaction. Previous studies, performed at room temperature, have shown that HU induces flexible bends, which can range from 0° to 180° with equal probability.[43,67] An increase in temperature could bias the bending angle distribution toward larger bending angles as the energy barrier required to bend the DNA is decreased. The observed increase in compaction could thus be a result of enhanced bending at higher temperatures. At 37 °C, the bimodal behavior of HU persisted: the observed compaction reached a maximum at 400 nM, and at concentrations of >400 nM, the apparent persistence length increased. The stiffening regime is, however, less pronounced compared to that at 23 °C as the apparent persistence length reached a maximum of 10.7 ± 0.3 nm at 1600 nM (compared to an L_p of 20.1 ± 0.4 nm at 23 °C). As the molecular mechanism underlying the stiffening mode is not understood, it is difficult to explain what causes the difference in stiffening at different temperatures. Possibly, the increased flexibility of the DNA at 37 °C effectively counteracts the stiffening effect of the HU filaments. Also, protein−protein interactions could be affected by temperature, influencing the side-by-side binding of HU proteins, which causes the observed stiffening. A smaller distribution of bending angles could also cause a less tight packing of the proteins on the DNA within the stiffening regime, causing a less pronounced stiffening effect, as observed. Indeed, it has been suggested that a flexible bending angle is needed for tight packing of proteins along the DNA.[11]

The increase in the flexibility of DNA at increased physiologically relevant temperatures is important when aiming to understand chromatin organization *in vivo*. It not only leads to a more compact configuration of the genomic DNA but also can have an important effect on cellular processes such as gene regulation. As DNA structure and topology are temperature-dependent, this may affect gene expression on a global level.[68] DNA supercoiling is proposed to act as a global regulator as it changes in response to environmental conditions and affects the expression of many genes.[69] Analogous to supercoiling, temperature-dependent DNA flexibility (and associated local changes in twist) and global compaction could provide a mechanism for temperature sensitive gene regulation.

■ ASSOCIATED CONTENT

Supporting Information

Table S1, Figures S1−S9, and supporting references. This material is available free of charge via the Internet at http://pubs.acs.org.

■ AUTHOR INFORMATION

Corresponding Author

*Telephone: +31 715275605. Fax: +31 715274357. E-mail: rtdame@chem.leidenuniv.nl.

Funding

This research was financially supported through a VIDI grant from The Netherlands Organization for Scientific Research (864.08.001 to R.Th.D.).

Notes

The authors declare no competing financial interest.

■ ACKNOWLEDGMENTS

We thank H. Duine and R. Shahapure for conducting preliminary experiments and Mariliis Tark-Dame and Frédéric Crémazy for comments on the manuscript. We thank E. de Waal for providing the pBTH154 plasmid.

■ REFERENCES

(1) Peters, J. P., III, and Maher, L. J. (2010) DNA curvature and flexibility in vitro and in vivo. *Q. Rev. Biophys. 43*, 23−63.

(2) Williams, L. D., and Maher, L. J., III (2000) Electrostatic mechanisms of DNA deformation. *Annu. Rev. Biophys. Biomol. Struct. 29*, 497−521.

(3) Garcia, H. G., Grayson, P., Han, L., Inamdar, M., Kondev, J., Nelson, P. C., Phillips, R., Widom, J., and Wiggins, P. A. (2007) Biological consequences of tightly bent DNA: The other life of a macromolecular celebrity. *Biopolymers 85*, 115−130.

(4) Luijsterburg, M. S., White, M. F., van Driel, R., and Dame, R. T. (2008) The major architects of chromatin: Architectural proteins in bacteria, archaea and eukaryotes. *Crit. Rev. Biochem. Mol. Biol. 43*, 393−418.

(5) Luger, K., Mader, A. W., Richmond, R. K., Sargent, D. F., and Richmond, T. J. (1997) Crystal structure of the nucleosome core particle at 2.8 Å resolution. *Nature 389*, 251−260.

(6) Reeve, J. N., Bailey, K. A., Li, W.-t., Marc, F., Sandman, K., and Soares, D. J. (2004) Archaeal histones: Structures, stability and DNA binding. *Biochem. Soc. Trans. 32*, 227−230.

(7) Maruyama, H., Harwood, J. C., Moore, K. M., Paszkiewicz, K., Durley, S. C., Fukushima, H., Atomi, H., Takeyasu, K., and Kent, N. A. (2013) An alternative beads-on-a-string chromatin architecture in *Thermococcus kodakarensis*. *EMBO Rep. 14*, 711−717.

(8) McCauley, M., Hardwidge, P. R., Maher, L. J., III, and Williams, M. C. (2005) Dual binding modes for an HMG domain from human HMGB2 on DNA. *Biophys. J. 89*, 353−364.

(9) Dame, R. T. (2005) The role of nucleoid-associated proteins in the organization and compaction of bacterial chromatin. *Mol. Microbiol. 56*, 858−870.

(10) Luijsterburg, M. S., Noom, M. C., Wuite, G. J., and Dame, R. T. (2006) The architectural role of nucleoid-associated proteins in the organization of bacterial chromatin: A molecular perspective. *J. Struct. Biol. 156*, 262−272.

(11) Driessen, R. P. C., Meng, H., Suresh, G., Shahapure, R., Lanzani, G., Priyakumar, U. D., White, M. F., Schiessel, H., van Noort, J., and

Dame, R. T. (2013) Crenarchaeal chromatin proteins Cren7 and Sul7 compact DNA by inducing rigid bends. *Nucleic Acids Res. 41*, 196−205.
(12) Perez-Martin, J., Rojo, F., and de Lorenzo, V. (1994) Promoters responsive to DNA bending: A common theme in prokaryotic gene expression. *Microbiol. Rev. 58*, 268−290.
(13) Saiz, L., and Vilar, J. M. (2006) DNA looping: The consequences and its control. *Curr. Opin. Struct. Biol. 16*, 344−350.
(14) Becker, N. A., Kahn, J. D., and Maher, L. J., III (2005) Bacterial repression loops require enhanced DNA flexibility. *J. Mol. Biol. 349*, 716−730.
(15) Becker, N. A., Kahn, J. D., and Maher, L. J., III (2007) Effects of nucleoid proteins on DNA repression loop formation in *Escherichia coli*. *Nucleic Acids Res. 35*, 3988−4000.
(16) Czapla, L., Peters, J. P., Rueter, E. M., Olson, W. K., and Maher, L. J., III (2011) Understanding apparent DNA flexibility enhancement by HU and HMGB architectural proteins. *J. Mol. Biol. 409*, 278−289.
(17) Zhang, Y., McEwen, A. E., Crothers, D. M., and Levene, S. D. (2006) Analysis of in-vivo LacR-mediated gene repression based on the mechanics of DNA looping. *PLoS One 1*, e136.
(18) Geanacopoulos, M., Vasmatzis, G., Zhurkin, V. B., and Adhya, S. (2001) Gal repressosome contains an antiparallel DNA loop. *Nat. Struct. Biol. 8*, 432−436.
(19) Cloutier, T. E., and Widom, J. (2004) Spontaneous sharp bending of double-stranded DNA. *Mol. Cell 14*, 355−362.
(20) Vafabakhsh, R., and Ha, T. (2012) Extreme bendability of DNA less than 100 base pairs long revealed by single-molecule cyclization. *Science 337*, 1097−1101.
(21) Yan, J., and Marko, J. F. (2004) Localized single-stranded bubble mechanism for cyclization of short double helix DNA. *Phys. Rev. Lett. 93*, 108108.
(22) Forties, R. A., Bundschuh, R., and Poirier, M. G. (2009) The flexibility of locally melted DNA. *Nucleic Acids Res. 37*, 4580−4586.
(23) Wiggins, P. A., Phillips, R., and Nelson, P. C. (2005) Exact theory of kinkable elastic polymers. *Phys. Rev. E: Stat., Nonlinear, Soft Matter Phys. 71*, 021909.
(24) Vologodskii, A., and Frank-Kamenetskii, M. D. (2013) Strong bending of the DNA double helix. *Nucleic Acids Res. 41*, 6785−6792.
(25) Altan-Bonnet, G., Libchaber, A., and Krichevsky, O. (2003) Bubble dynamics in double-stranded DNA. *Phys. Rev. Lett. 90*, 138101.
(26) Cloutier, T. E., and Widom, J. (2005) DNA twisting flexibility and the formation of sharply looped protein-DNA complexes. *Proc. Natl. Acad. Sci. U.S.A. 102*, 3645−3650.
(27) Geggier, S., Kotlyar, A., and Vologodskii, A. (2011) Temperature dependence of DNA persistence length. *Nucleic Acids Res. 39*, 1419−1426.
(28) Gadgil, M., Kapur, V., and Hu, W. S. (2005) Transcriptional response of *Escherichia coli* to temperature shift. *Biotechnol. Prog. 21*, 689−699.
(29) Tachdjian, S., and Kelly, R. M. (2006) Dynamic metabolic adjustments and genome plasticity are implicated in the heat shock response of the extremely thermoacidophilic archaeon *Sulfolobus solfataricus*. *J. Bacteriol. 188*, 4553−4559.
(30) Battesti, A., Majdalani, N., and Gottesman, S. (2011) The RpoS-mediated general stress response in *Escherichia coli*. *Annu. Rev. Microbiol. 65*, 189−213.
(31) Dame, R. T. Architectural roles of H-NS and HU in DNA compaction and transcription regulation. Ph.D. Thesis, Leiden University, Leiden, The Netherlands, 2003.
(32) Moolenaar, G. F., Visse, R., Ortiz-Buysse, M., Goosen, N., and van de Putte, P. (1994) Helicase motifs V and VI of the *Escherichia coli* UvrB protein of the UvrABC endonuclease are essential for the formation of the preincision complex. *J. Mol. Biol. 240*, 294−307.
(33) She, Q., Singh, R. K., Confalonieri, F., Zivanovic, Y., Allard, G., Awayez, M. J., Chan-Weiher, C. C., Clausen, I. G., Curtis, B. A., De Moors, A., Erauso, G., Fletcher, C., Gordon, P. M., Heikamp-de Jong, I., Jeffries, A. C., Kozera, C. J., Medina, N., Peng, X., Thi-Ngoc, H. P., Redder, P., Schenk, M. E., Theriault, C., Tolstrup, N., Charlebois, R. L., Doolittle, W. F., Duguet, M., Gaasterland, T., Garrett, R. A., Ragan, M. A., Sensen, C. W., and Van der Oost, J. (2001) The complete genome of the crenarchaeon *Sulfolobus solfataricus* P2. *Proc. Natl. Acad. Sci. U.S.A. 98*, 7835−7840.
(34) Ramos, C. R., Abreu, P. A., Nascimento, A. L., and Ho, P. L. (2004) A high-copy T7 *Escherichia coli* expression vector for the production of recombinant proteins with a minimal N-terminal His-tagged fusion peptide. *Braz. J. Med. Biol. Res. 37*, 1103−1109.
(35) Bentley, S. D., Chater, K. F., Cerdeno-Tarraga, A. M., Challis, G. L., Thomson, N. R., James, K. D., Harris, D. E., Quail, M. A., Kieser, H., Harper, D., Bateman, A., Brown, S., Chandra, G., Chen, C. W., Collins, M., Cronin, A., Fraser, A., Goble, A., Hidalgo, J., Hornsby, T., Howarth, S., Huang, C. H., Kieser, T., Larke, L., Murphy, L., Oliver, K., O'Neil, S., Rabbinowitsch, E., Rajandream, M. A., Rutherford, K., Rutter, S., Seeger, K., Saunders, D., Sharp, S., Squares, R., Squares, S., Taylor, K., Warren, T., Wietzorrek, A., Woodward, J., Barrell, B. G., Parkhill, J., and Hopwood, D. A. (2002) Complete genome sequence of the model actinomycete *Streptomyces coelicolor* A3(2). *Nature 417*, 141−147.
(36) Laurens, N., Bellamy, S. R., Harms, A. F., Kovacheva, Y. S., Halford, S. E., and Wuite, G. J. (2009) Dissecting protein-induced DNA looping dynamics in real time. *Nucleic Acids Res. 37*, 5454−5464.
(37) Reif, R. (1985) *The Fundamentals of Statistical and Thermal Physics*, McGraw-Hill, New York.
(38) Happel, J., and Brenner, H. (1983) *Low Reynolds Number Hydrodynamics*, Kluwer Academic Publishers, Dordrecht, The Netherlands.
(39) Schaffer, E., Norrelykke, S. F., and Howard, J. (2007) Surface forces and drag coefficients of microspheres near a plane surface measured with optical tweezers. *Langmuir 23*, 3654−3665.
(40) Seol, Y., Li, J., Nelson, P. C., Perkins, T. T., and Betterton, M. D. (2007) Elasticity of short DNA molecules: Theory and experiment for contour lengths of 0.6−7 μm. *Biophys. J. 93*, 4360−4373.
(41) Risken, H. (1989) *The Fokker-Planck Equation: Methods of Solution and Applications*, Springer, Berlin.
(42) Geggier, S., and Vologodskii, A. (2010) Sequence dependence of DNA bending rigidity. *Proc. Natl. Acad. Sci. U.S.A. 107*, 15421−15426.
(43) van Noort, J., Verbrugge, S., Goosen, N., Dekker, C., and Dame, R. T. (2004) Dual architectural roles of HU: Formation of flexible hinges and rigid filaments. *Proc. Natl. Acad. Sci. U.S.A. 101*, 6969−6974.
(44) Kulić, I. M., Mohrbach, H., Lobaskin, V., Thaokar, R., and Schiessel, H. (2005) Apparent persistence length renormalization of bent DNA. *Phys. Rev. E: Stat., Nonlinear, Soft Matter Phys. 72*, 041905.
(45) Lee, N. K., Park, J. S., Johner, A., Obukhov, S., Hyon, J. Y., Lee, K. J., and Hong, S. C. (2008) Elasticity of cisplatin-bound DNA reveals the degree of cisplatin binding. *Phys. Rev. Lett. 101*, 248101.
(46) Galburt, E. A., Tomko, E. J., Stump, W. T., and Ruiz Manzano, A. (2014) Force-dependent melting of supercoiled DNA at thermophilic temperatures. *Biophys. Chem. 187−188C*, 23−28.
(47) Driessen, R. P. C., and Dame, R. T. (2011) Nucleoid-associated proteins in Crenarchaea. *Biochem. Soc. Trans. 39*, 116−121.
(48) Driessen, R. P. C., and Dame, R. T. (2013) Structure and dynamics of the crenarchaeal nucleoid. *Biochem. Soc. Trans. 41*, 321−325.
(49) Brock, T. D., Brock, K. M., Belly, R. T., and Weiss, R. L. (1972) *Sulfolobus*: A new genus of sulfur-oxidizing bacteria living at low pH and high temperature. *Arch. Mikrobiol, 84*, 54−68.
(50) Feng, Y., Yao, H., and Wang, J. (2010) Crystal structure of the crenarchaeal conserved chromatin protein Cren7 and double-stranded DNA complex. *Protein Sci. 19*, 1253−1257.
(51) Zhang, Z., Gong, Y., Guo, L., Jiang, T., and Huang, L. (2010) Structural insights into the interaction of the crenarchaeal chromatin protein Cren7 with DNA. *Mol. Microbiol. 76*, 749−759.
(52) Gao, Y. G., Su, S. Y., Robinson, H., Padmanabhan, S., Lim, L., McCrary, B. S., Edmondson, S. P., Shriver, J. W., and Wang, A. H. (1998) The crystal structure of the hyperthermophile chromosomal protein Sso7d bound to DNA. *Nat. Struct. Biol. 5*, 782−786.
(53) Baumann, H., Knapp, S., Lundbäck, T., Ladenstein, R., and Härd, T. (1994) Solution structure and DNA-binding properties of a

thermostable protein from the archaeon *Sulfolobus solfataricus*. *Nat. Struct. Biol. 1*, 808−819.
(54) Guo, L., Feng, Y., Zhang, Z., Yao, H., Luo, Y., Wang, J., and Huang, L. (2008) Biochemical and structural characterization of Cren7, a novel chromatin protein conserved among Crenarchaea. *Nucleic Acids Res. 36*, 1129−1137.
(55) Laurens, N., Driessen, R. P. C., Heller, I., Vorselen, D., Noom, M. C., Hol, F. J. H., White, M. F., Dame, R. T., and Wuite, G. J. L. (2012) Alba shapes the archaeal genome using a delicate balance of bridging and stiffening the DNA. *Nat. Commun. 3*, 1328.
(56) McGhee, J. D., and von Hippel, P. H. (1974) Theoretical aspects of DNA-protein interactions: Co-operative and non-co-operative binding of large ligands to a one-dimensional homogeneous lattice. *J. Mol. Biol. 86*, 469−489.
(57) Agback, P., Baumann, H., Knapp, S., Ladenstein, R., and Hard, T. (1998) Architecture of nonspecific protein-DNA interactions in the Sso7d-DNA complex. *Nat. Struct. Biol. 5*, 579−584.
(58) Skoko, D., Wong, B., Johnson, R. C., and Marko, J. F. (2004) Micromechanical analysis of the binding of DNA-bending proteins HMGB1, NHP6A, and HU reveals their ability to form highly stable DNA-protein complexes. *Biochemistry 43*, 13867−13874.
(59) Nir, G., Lindner, M., Dietrich, H. R., Girshevitz, O., Vorgias, C. E., and Garini, Y. (2011) HU protein induces incoherent DNA persistence length. *Biophys. J. 100*, 784−790.
(60) Dame, R. T., Hall, M. A., and Wang, M. D. (2013) Single-Molecule Unzipping Force Analysis of HU-DNA Complexes. *ChemBioChem 14*, 1954−1957.
(61) Yakovchuk, P., Protozanova, E., and Frank-Kamenetskii, M. D. (2006) Base-stacking and base-pairing contributions into thermal stability of the DNA double helix. *Nucleic Acids Res. 34*, 564−574.
(62) Peters, J. P., Yelgaonkar, S. P., Srivatsan, S. G., Tor, Y., and James Maher, L., III (2013) Mechanical properties of DNA-like polymers. *Nucleic Acids Res. 41*, 10593−10604.
(63) Meyer, S., Jost, D., Theodorakopoulos, N., Peyrard, M., Lavery, R., and Everaers, R. (2013) Temperature dependence of the DNA double helix at the nanoscale: Structure, elasticity, and fluctuations. *Biophys. J. 105*, 1904−1914.
(64) Peters, W. B., Edmondson, S. P., and Shriver, J. W. (2004) Thermodynamics of DNA binding and distortion by the hyperthermophile chromatin protein Sac7d. *J. Mol. Biol. 343*, 339−360.
(65) Lundbäck, T., and Härd, T. (1996) Salt Dependence of the Free Energy, Enthalpy, and Entropy of Nonsequence Specific DNA Binding. *J. Phys. Chem. 100*, 17690−17695.
(66) Chen, L., Zhang, J. L., Yu, L. Y., Zheng, Q. C., Chu, W. T., Xue, Q., Zhang, H. X., and Sun, C. C. (2012) Influence of hyperthermophilic protein Cren7 on the stability and conformation of DNA: Insights from molecular dynamics simulation and free energy analysis. *J. Phys. Chem. B 116*, 12415−12425.
(67) Swinger, K. K., Lemberg, K. M., Zhang, Y., and Rice, P. A. (2003) Flexible DNA bending in HU-DNA cocrystal structures. *EMBO J. 22*, 3749−3760.
(68) Travers, A. (2013) Dynamic DNA underpins chromosome dynamics. *Biophys. J. 105*, 2235−2237.
(69) Hatfield, G. W., and Benham, C. J. (2002) DNA topology-mediated control of global gene expression in *Escherichia coli*. *Annu. Rev. Genet. 36*, 175−203.